PHYSICAL REVIEW C, VOLUME 62, 041001(R)

# Four-body distorted wave theory for halo excitations

S. N. Ershov,* B. V. Danilin,† and J. S. Vaagen
*SENTEF, Department of Physics, University of Bergen, Bergen, Norway*
(Received 6 April 2000; published 19 September 2000)

A microscopic approach to breakup reactions into the low-energy continuum of Borromean two-neutron halo nuclei is developed, taking quantum-mechanically into account both Coulomb and nuclear dissociation, simultaneously. The crucial role of both elastic and inelastic fragmentation is demonstrated for $^6$He breakup on C and Pb targets at intermediate energies, for kinematically complete experiments. Recent GSI experimental data are for the first time analyzed quantitatively and reveal a rich and complex interplay of reaction mechanisms and low-lying halo excitations.

PACS number(s): 21.45.+v, 24.10.Eq, 25.70.De, 25.70.Mn

Recently [1] we demonstrated within a microscopic four-body distorted wave theory that in diffractive (elastic) breakup of Borromean halo nuclei on proton target, the correlated continuum excitations play a crucial role for fragment momentum distributions. We have extended this approach to breakup reactions on heavier targets taking into account the presence of different reaction mechanisms leading to elastic and inelastic fragmentations, i.e., when the target remains in the ground or goes to excited states, respectively.

The most explored Borromean nucleus, both theoretically and experimentally is $^6$He, for which nevertheless, the question of the nature of low-lying soft modes is still under discussion since controversy of theoretical analysis [2–5] and recent experimental results [6] remains. Below we present the first study of continuum excitations for both elastic and inelastic $^6$He breakup on $^{12}$C (nuclear interaction dominates) and $^{208}$Pb (Coulomb dissociation is the main process) targets and compare theory with recent experimental data from GSI [6] at a collision energy of 240 MeV/nucleon. Other breakup scenarios are discussed in [7]

The reaction amplitude of the breakup reaction $a+A \rightarrow \alpha+n_1+n_2+A'$ involving the collision of projectile $a$ (two-neutron halo) and target $A$ includes in prior representation the exact continuum wave functions $\Psi^{(-)}_{A'}(\boldsymbol{k}_x,\boldsymbol{k}_y,\boldsymbol{k}_f)$ which describe the relative motion of halo fragments and target in excited state $A'$. Jacobi vectors $(\boldsymbol{k}_x,\boldsymbol{k}_y)$ characterize the relative motion of the three projectile breakup fragments, and $\boldsymbol{k}_f$ the relative target-projectile center-of-mass motion [2,8]. To get $\Psi^{(-)}_{A'}$ some approximations are required. We make approximations at the level of the reaction mechanism but treat the three-body structure of the halo projectile in a consistent way keeping the characteristics of the halo structure. These are contained directly in the halo ground state wave function and in the low-lying excitation spectra where strength concentration of transitions with different multipolarities, so called ''soft modes,'' are formed. If there is no direct knockout of a projectile fragment we cannot neglect any of the mutual interactions. All projectile fragments take similar parts in the interaction process. This is realized for the soft part of a halo spectrum where relative fragment velocities are small and restricted kinematically by the low excitation energy $E^*$. At low $E^*$ there are no spectator particles. Also the reaction should be fast and the loss of energy has to be small compared with the initial collision energy. Hence, we factorize the exact scattering wave function explicitly extracting a wave function of the excited projectile. Thus the reaction amplitude can be written as

$$\langle \chi^{(-)}_{A'}(\boldsymbol{k}_f)\Phi_{A'}\Psi^{(-)}(\boldsymbol{k}_x,\boldsymbol{k}_y)|V_{aA}|\Psi_0\Phi_0\chi^{(+)}_0(\boldsymbol{k}_i)\rangle,$$

where $\Psi^{(-)}(\boldsymbol{k}_x,\boldsymbol{k}_y)$ is a continuum three-body wave function of the halo system, $\Psi_0$ is the halo ground state, while $\chi^{(\pm)}_{A'}(\boldsymbol{k}_{i,f})$ are distorted waves describing relative motion of projectile and target in state $\Phi_{A'}$. The transition potential $V_{aA}=\Sigma_{p,t}V_{p,t}$ which governs the fragmentation process in the breakup reactions is composed of effective $NN$ interactions $V_{p,t}$ between projectile $p$ and target $t$ nucleons. The post and prior forms of the breakup amplitude are equal in our approximation since the decomposition of the Hamiltonian in perturbed and unperturbed parts is the same for initial and final channels. According to this approach the nature of the breakup is inelastic excitations of the projectile directly to the continuum. Whether this continuum state will be resonant or nonresonant depends on the final state interactions between the fragments.

To calculate the reaction amplitude the bound $\Psi_0$ and continuum $\Psi^{(-)}(\boldsymbol{k}_x,\boldsymbol{k}_y)$ wave functions have to be precomputed. For the $^6$He nucleus the essential halo structure has been obtained in the framework of a three-body $\alpha+N+N$ model [2,9]. In this model, the total wave function is represented by a product of wave functions describing the internal structure of the $\alpha$ core and the relative motion of three interacting constituents. The method of hyperspherical harmonics (HH) [2] has been used to treat the three-body dynamics for both bound and scattering states. This allowed us to provide [10,8,1] a comprehensive description of a variety of data for $A=6$ systems. For the present calculations the HH method has been extended in an effective way to include both the core polarization [2] and two-neutron-exchange with the core by using the core density dependent $NN$ interaction, which includes repulsion inside the core in the Pauli-

*Permanent address: JINR, Dubna, Russia.
†Permanent address: RRC, The Kurchatov Institute, Moscow, Russia.

 

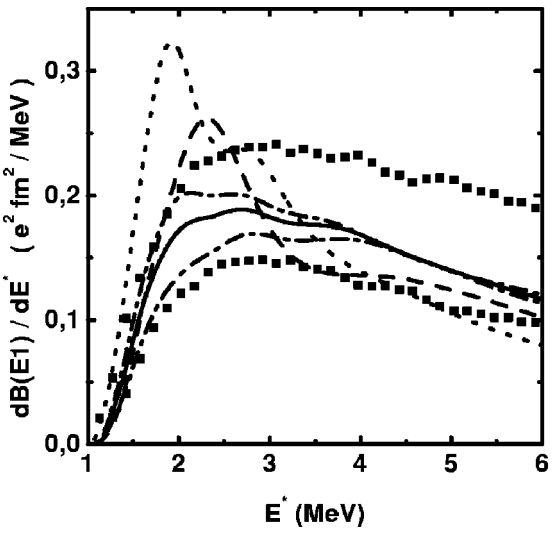


FIG. 1. Dipole strength distributions for $^6$He. Solid and dashed-dotted lines show the distribution and theoretical uncertainty in the present improved calculations. Dashed and dotted lines are for theoretical calculations from [2] and [5], respectively. Dark squares are experimentally derived boundaries from [6].

forbidden partial states. Details of the method will be published elsewhere. The Feshbach reduction to inactive subspace was used, and in all partial states we have reduced the initial $K\sim 40$ hyperharmonic space (enough for practical convergence) to $K\sim 10$, which gives the same results as a strict calculation in the large initial space. Exchange effects cause a difference in dipole strength functions calculated in the simple [2,5] and improved cluster models, but affect the ground state wave function very little. In present calculations we used the improved cluster wave functions which give the dipole strength distribution (solid line in Fig. 1) within the GSI experimental data. The boundaries of theoretical uncertainties, within which our qualitative conclusions certainly hold, are shown by dash-dotted lines in Fig. 1

TABLE I. Theoretical (integrated over excitation energy $E^*\leqslant 10$ MeV) cross sections (mb) for inelastic excitation of $^6$He at 240 MeV/nucleon on $^{208}$Pb and $^{12}$C targets. $N$ ($C$) labels the calculations with purely nuclear (Coulomb) forces. Experimental data [6] include cross sections up to $E^*\leqslant 12.3$ MeV.

| | Total | Elastic | Inelastic | $0^+$ | $1^-$ | $2^+$ | $2^+_{res}$ |
|---|---|---|---|---|---|---|---|
| $^{208}$Pb | | | | | | | |
| $N$ | 218 | 73 | 145 | 20 | 112 | 87 | 41 |
| $C$ | 299 | 267 | 32 | 0 | 293 | 1.3 | 0.4 |
| $N+C$ | 480 | 333 | 147 | 20 | 378 | 82 | 40 |
| exp [6] | 650±110 | | | | | | 14±4 |
| $^{12}$C | | | | | | | |
| $N$[a] | 16.9 | 8.6 | 8.3 | 1.3 | 6.9 | 8.7 | 4.5 |
| $C$[a] | 1.9 | 1.7 | 0.2 | 0 | 1.9 | 0.02 | 0.01 |
| $(N+C)$[a] | 16.8 | 9.3 | 7.5 | 1.3 | 7.2 | 8.4 | 4.4 |
| $(N+C)$[b] | 20.6 | 11.0 | 9.6 | 2.7 | 9.2 | 8.7 | 4.5 |
| exp [6] | 30±5 | | | | | | 4±0.8 |

[a]Optical potential used in calculations from Ref. [15].
[b]Optical potential used in calculations from Ref. [16].

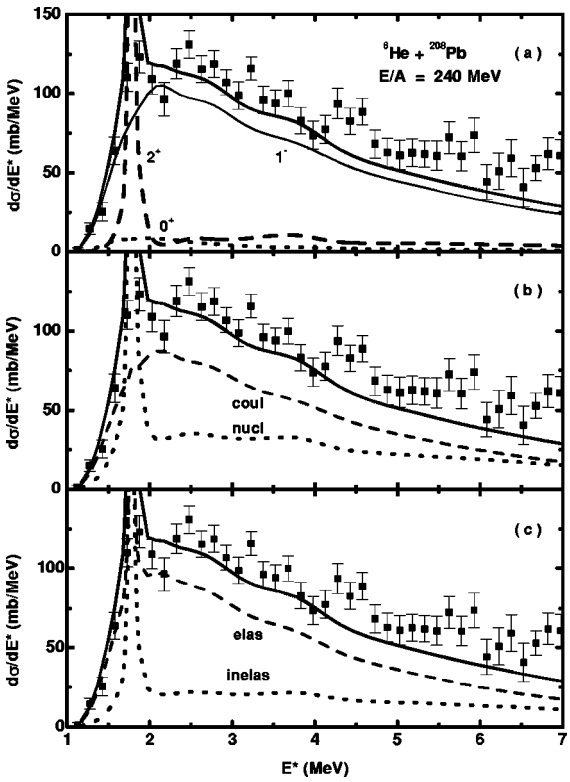


FIG. 2. Comparison of the theoretical $^6$He excitation spectrum (thick solid line) for $^6$He+$^{208}$Pb breakup at 240 MeV/nucleon with experimental data [6]. (a) The thin solid, dashed, and dotted lines show the dipole $1^-$, quadrupole $2^+$, and monopole $0^+$ contributions. (b) Dashed (dotted) lines show calculations with only nuclear (Coulomb) interactions. (c) Dashed (dotted) lines are contributions from elastic (inelastic) fragmentation.

It is important to underline that in the calculations of the continuum wave functions $\Psi^{(-)}(\boldsymbol{k}_x,\boldsymbol{k}_y)$ the final state interaction (the pair interactions between all projectile constituents) is fully taken into account.

For a consistent treatment of electromagnetic dissociation Coulomb and nuclear interactions have to be treated on equal footing. The interaction $V_{pt}$ between projectile and target nucleons has a short-range part due to strong forces but also includes the Coulomb repulsion when both nucleons are protons. This allows quantum-mechanical calculations of nuclear and Coulomb excitations including their interference, without artificial separation in different mechanisms.

Inclusive cross sections include both elastic and inelastic breakup reactions. To single out these contributions we use the method of Refs. [11–13]. Thus, the inclusive cross section $\sigma=\sigma_{el}+\sigma_{in}$ is decomposed into elastic $\sigma_{el}$ and inelastic $\sigma_{in}$ parts given by

$$\sigma_{el}=\frac{(2\pi)^4}{\hbar v_i}\int d\boldsymbol{k}_x d\boldsymbol{k}_y d\boldsymbol{k}_f \delta(\varepsilon_i-\varepsilon_f-E^*) \times|\langle\chi_0^{(-)}(\boldsymbol{k}_f)\Phi_0\Psi^{(-)}(\boldsymbol{k}_x,\boldsymbol{k}_y)|V_{aA}|\Psi_0\Phi_0\chi_0^{(+)}(\boldsymbol{k}_i)\rangle|^2,$$

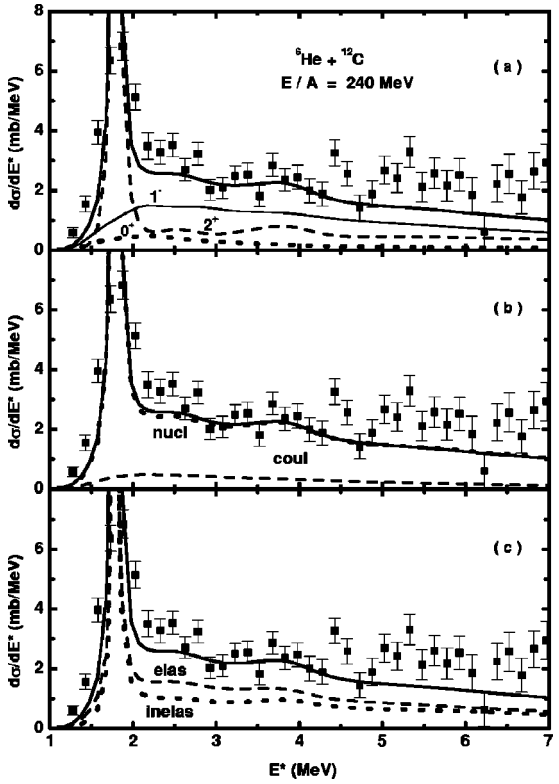


FIG. 3. The same as in Fig. 2 but for $^6$He+$^{12}$C reaction.

$$\sigma_{in}=\frac{(2\pi)^4}{\hbar v_i}\int d\boldsymbol{k}_x d\boldsymbol{k}_y \int d\boldsymbol{r}\frac{1}{\pi}(-\mathrm{Im}\,U_{aA}(r)) \times|\langle G_{opt}(\boldsymbol{r},\omega)\Phi_0\Psi^{(-)}(\boldsymbol{k}_x,\boldsymbol{k}_y)|V_{aA}|\Psi_0\Phi_0\chi_0^{(+)}(\boldsymbol{k}_i)\rangle|^2,$$

where $\varepsilon_{i,f}$ are the kinetic energies of relative center-of-mass motion in the channels, $\omega=\varepsilon_i-E^*$, and the optical-model Green's function $G_{opt}(\boldsymbol{r},\boldsymbol{r}',\omega)$ is the solution of the Schrödinger equation with optical potential $U_{aA}$.

The calculations in the impulse approximation used an effective *NN* interaction with the parametrization of [14] for the nucleon-nucleon *t* matrix. Optical potentials [15] for $^{12}$C scattering on $^{12}$C and $^{208}$Pb at 200 MeV/nucleon were used with radius parameters scaled to the number of nucleons in $^6$He.

Table I shows total theoretical cross sections integrated over excitation energy up to 10 MeV for inelastic excitations of $^6$He on $^{208}$Pb and $^{12}$C targets. Figures 2 and 3 show the corresponding spectra compared with experimental data [6]. The calculations correctly describe absolute values and spectral shape for both reactions, in spite of their different reaction mechanisms. Still theory underestimates the total cross sections somewhat, caused by insufficient contributions at higher $E^*$. In this respect the calculations can be improved by including excitations with higher multipolarities [8] currently not taken into account. We draw attention to the increase in the nuclear breakup going from light to heavy targets in our calculations by a factor of about 10 while calculations in [6,7] only gave a factor of 4. This difference has to be clarified.

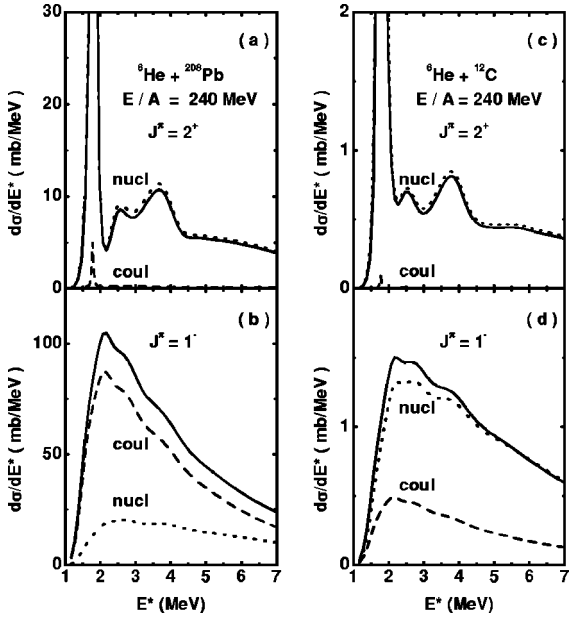


FIG. 4. Quadrupole (a) and dipole (b) excitations on $^{208}$Pb, and quadrupole (c) and dipole (d) excitations on $^{12}$C. Dashed (dotted) lines show calculations with only Coulomb (nuclear) interactions.

The contributions [Fig. 2(a)] to inclusive spectra on a lead target from different multipole excitations in $^6$He display a small monopole contribution, the dipole dominates and the well-known three-body $2^+$ resonance at 1.8 MeV is strongly excited (total cross section $\sim$40 mb). Since the calculated resonance width ($\sim$60 keV) is less than experiment ($\sim$113 keV) and no energy averaging with experimental resolution performed, the theoretical peak cross section exceeds the experimental one. The steep cross section increase at threshold is completely due to dipole excitations. Figure 2(b) shows the cross sections for calculations with only Coulomb or nuclear interaction. Coulomb dissociation dominates, but cannot alone describe absolute values of experimental data. Applying the semiclassical method to our dipole strength function gives $\sim$420 mb for a cutoff minimum impact parameter of 9.5 fm. Quantum calculations when only the Coulomb part of optical potentials is present gave $\sim$400 mb for the dipole elastic cross section. The cross section contributions from elastic and inelastic fragmentation are shown in Fig. 2(c). Although the elastic fragmentation dominates the low-energy part of the spectrum, for a quantitative description both contributions have to be taken into account simultaneously. The elastic fragmentation cross section decreases rapidly with energy while the inelastic stays rather flat. In total, $\sigma_{in}$ on $^{208}$Pb contributes about 30% of total cross section for $E^*\leqslant 10$ MeV.

Figure 3 shows comparisons of theoretical calculations with experimental data [6] for $^6$He+$^{12}$C at 240 MeV/nucleon. The peak, the most pronounced feature in the spectrum, is again due to excitation of the $2^+$ resonance [Fig. 3(a)] with total cross section $\sim$4 mb. Above the resonance, in the flat part of the spectrum, approximately half of the cross section is due to dipole, a third is quadrupole, and the rest are monopole excitations. On the carbon target the in-

clusive excitation spectrum is completely defined by nuclear interaction [Fig 3(b)] and the contributions from elastic and inelastic fragmentations are approximately equal [Fig. 3(b)].

Figure 4 addresses in particular the quadrupole (a),(c) and dipole (b),(d) excitations of $^{6}$He for reactions on $^{12}$C and $^{208}$Pb targets. For quadrupole transitions the Coulomb interaction is not important. The dipole nuclear fragmentation on $^{12}$C is more than 2 times the Coulomb. Its cross section is roughly increased by one order of magnitude for $^{208}$Pb, but dipole Coulomb dissociation is increased by more then two orders of magnitude. This factor is similar to the square of the ratio of the target charges and is expected for pure Coulomb excitations. When both interactions are present the picture becomes more complex: there is a destructive interference in the internal region and Coulomb excitation in the outer.

To check sensitivity to optical potentials the calculations for fragmentation on $^{12}$C have also been done with the potential from Ref. [16]. This optical potential has a ''shallow'' imaginary part and may represent a reasonable variation of the potential family. Calculations show only minor changes for quadrupole transitions while dipole cross sections are increased by 30%, and contribution from monopole excitations is doubled. The total cross section for $E^{*} \leqslant 10$ MeV is increased by 20%. It is clearly demonstrated that the use of a transparent potential influences the excitations concentrated more deeply inside the nucleus more strongly.

In conclusion, we have extended our microscopic four-body DWIA theory for two-neutron halo breakup reactions to account for both elastic and inelastic breakup leading to low-lying halo excitations. Within this approach the Coulomb and nuclear dissociations are included in a consistent way which accounts for Coulomb-nuclear interference. The method of hyperspherical harmonics is used for a consistent description of genuine features of the halo bound state and final state interactions between all halo fragments. The procedure can be applied to analyze kinematically complete experiments, which allow reconstruction of the halo excitation spectrum, and single out the events carrying valuable information on correlations specific to two-neutron halo systems. The model was used to analyze recent experimental data [6] on $^{6}$He fragmentation at 240 MeV/nucleon on $^{12}$C and $^{208}$Pb targets. In addition to a good simultaneous description of absolute cross sections and excitation spectra for both reactions, new insight on the interplay of reaction mechanisms and correlated continuum structure was obtained. The important role found for inelastic fragmentation and Coulomb-nuclear interference is consistent with experimental data. Application of the approach to other Borromean nuclei is in progress.

This work was done under financial support from the Bergen member of the RNBT Collaboration and BCPL project. B.D. and S.E. are thankful to the University of Bergen for hospitality. B.D. acknowledges support from RFBR Grant No. 99-02-17610. The authors are grateful to Professor M.V. Zhukov for useful discussions.

[1] S.N. Ershov *et al.*, Phys. Rev. Lett. **82**, 908 (1999).
[2] B.V. Danilin *et al.*, Nucl. Phys. **A632**, 383 (1998).
[3] A. Csótó, Phys. Rev. C **49**, 3035 (1994).
[4] S. Aoyaama, S. Mukai, K. Kato, and K. Ikeda, Prog. Theor. Phys. **93**, 99 (1995).
[5] A. Cobis, D. Fedorov, and A. Jensen, Phys. Rev. Lett. **79**, 2411 (1997).
[6] T. Aumann *et al.*, Phys. Rev. C **59**, 1252 (1999).
[7] G.F. Bertsch, K. Hencken, and H. Esbensen, Phys. Rev. C **57**, 1366 (1998).
[8] S.N. Ershov *et al.*, Phys. Rev. C **56**, 1483 (1997).
[9] M.V. Zhukov *et al.*, Phys. Rep. **231**, 151 (1993).
[10] B.V. Danilin *et al.*, Phys. Rev. C **43**, 2835 (1991).
[11] N. Austern and C.M. Vincent, Phys. Rev. C **23**, 1847 (1981).
[12] T. Udagawa and T. Tamura, Phys. Rev. C **24**, 1348 (1981).
[13] A. Kasano and M. Ichimura, Phys. Lett. **115B**, 81 (1982).
[14] M.A. Franey and W.G. Love, Phys. Rev. C **31**, 488 (1985).
[15] J.Y. Hostachy *et al.*, Nucl. Phys. **A490**, 441 (1988).
[16] M.E. Brandan, Phys. Rev. Lett. **60**, 784 (1988).